Assessing the 4f orbital participation in the Ln-C bonds of $[Li(THF)_4][Ln(C_6Cl_5)_4]$ (Ln = La, Ce)

Osvaldo Ordoñez, Xiaojuan Yu, Guang Wu, Jochen Autschbach*, and Trevor W. Hayton*

Department of Chemistry and Biochemistry, University of California Santa Barbara, Santa Barbara, CA 93106

Department of Chemistry, University at Buffalo, State University of New York, Buffalo, NY 14260

*To whom correspondence should be addressed. Email: jochena@buffalo.edu, hayton@chem.ucsb.edu

Abstract

Reaction of $[Ln(NO_3)_3(THF)_4]$ (Ln = La; Ce) with 4 equiv of LiC_6Cl_5 in Et_2O resulted in the formation of the homoleptic lanthanide-aryl "ate" complexes $[Li(THF)_4][La(C_6Cl_5)_4]$ ([Li][**1**]) and $[Li(THF)_4][Ce(C_6Cl_5)_4]$ ([Li][**2**]). These complexes represent the first isolated homoleptic perchlorophenyl complexes for the lanthanides. In the solid state, both [Li][**1**] and [Li][**2**] exhibit octa-coordinate lanthanide centers, with four Ln-C σ-bonds and four Cl→Ln dative interactions involving the *ortho*-Cl atoms of the C_6Cl_5 ligands. Despite this apparent steric saturation, both [Li][**1**] and [Li][**2**] are highly temperature sensitive and quickly decompose in solution at room temperature. Density functional calculations show that the Ln-C_{ipso} donation bonds feature only weak 4f participation (e.g., ~1% 4f weight for $[\mathbf{1}]^-$). Nonetheless, the ^{13}C chemical shift for the C_{ipso} nuclei of $[\mathbf{1}]^-$ includes ca. 8 ppm of deshielding from spin-orbit coupling effects from the 4f (and 5d) participation in its La-C bonds.

Introduction

Homoleptic lanthanide aryl complexes have a long and rich history.[1–5] The first structurally characterized example, $[Li(THF)_4][Lu(2,6\text{-}Me_2C_6H_3)_4]$, was isolated in 1972 by Hursthouse and co-workers.[2] Since that time, a large number homoleptic Ln aryl complexes have been reported in the literature. Many of these complexes utilize pendant donor groups to stabilize the Ln-C$_{aryl}$ bonds,[1,3,4] such as $[Ln(\eta^2\text{-}N,C\text{-}C_6H_4\text{-}o\text{-}CH_2NMe_2)_3]$ (Ln = Er, Yb, Lu, Y),[4] $[Ln(\eta^2\text{-}N,C\text{-}C_6H_4\text{-}o\text{-}CH(Me)NMe_2)_3]$ (Ln = Y, Dy, Nd, Sm),[1] $[Sm(\eta^2\text{-}N,C\text{-}C_6H_4\text{-}o\text{-}C(Me)_2NMe_2)_3]$,[1] and $[La\{(S,S,)\text{-Phebox-}^i\text{Pr}\}_3]$,[3] among others.[1,4,6–8] However, many solvent-stabilized Ln aryl complexes are also known, which do not feature stabilizing pendant donor groups. Among these examples are several $[Ln(Ar)_3(solvent)_x]$- and $[Ln(Ar)_2(solvent)_x]$-type complexes,[9–12] including $[Yb(C_6F_5)_2(THF)_4]$ and $[Eu(Dpp)_2(THF)_2]$ (Dpp = $2,6\text{-}Ph_2C_6H_3$).[11,12] These complexes are functionally homoleptic due to the lability of their solvent donor ligands. Yet, despite this rich history, there are no reported lanthanide complexes containing the perchlorophenyl ligand (C_6Cl_5), which is remarkable given the large number of homoleptic C_6Cl_5 complexes reported for the transition metals,[13–22] and more recently, the actinides.[23,24]

Previously, we and others have shown that ^{13}C NMR spectroscopy is a valuable tool to evaluate covalency in actinide-ligand bonding.[23–31] In particular, the ^{13}C chemical shifts of organometallic ligands have proven to be highly sensitive to the degree of 5f orbital participation in the An-C bonds. Actinide perchlorophenyl complexes have also proven useful in this regard.[23,24] For example, the C$_{ipso}$ chemical shift in the uranyl C_6Cl_5 complex $[Li(Et_2O)_2(THF)][UO_2(C_6Cl_5)_3]$ was found at 236.7 ppm. Calculations reveal a 62 ppm downfield spin-orbit (SO) induced shift due to the involvement of the 5f orbitals in the U-C bonding.[23] In contrast, this method of analysis has not been widely applied to the lanthanides. In one case, reported by Schelter and co-workers, an analysis of the ^{13}C NMR spectrum of $[Li(THF)_4][Ce^{IV}(\kappa^2$-*ortho*-oxa)(MBP)$_2]$ (*ortho*-oxa = dihydro-dimethyl-2-[4-(trifluoromethyl)phenyl]-oxazolide, MBP^{2-} = 2,2′-methylenebis(6-*tert*-butyl-4-methylphenolate)) reveals a calculated 40 ppm SO–induced shift for the C_{ipso} resonance, which is compelling evidence of 4f involvement in lanthanide(IV)-ligand bonding.[32] That said, to our knowledge this method has not been applied to Ln(III) organometallics.

In an effort to expand this method of analysis to lanthanide organometallics, we targeted the synthesis of two homoleptic lanthanide-aryl “ate” complexes $[Li(THF)_4][La(C_6Cl_5)_4]$ ([Li][**1**]) and $[Li(THF)_4][Ce(C_6Cl_5)_4]$ ([Li][**2**]). These complexes proved to be highly thermally sensitive; nonetheless, both complexes were characterized by X-ray crystallography and $^{13}C\{^1H\}$ NMR spectroscopy, and their electronic structures were examined by density functional theory (DFT) with a relativistic Hamiltonian.

Results and Discussion

Synthesis and Characterization. Reaction of $[La(NO_3)_3(THF)_4]$ with 4 equiv of LiC_6Cl_5[33] in cold Et_2O (-25 °C) resulted in immediate formation of an orange-yellow solution, concomitant with the deposition of copious amounts of tan precipitate. Work-up of reaction mixture afforded $[Li(THF)_4][La(C_6Cl_5)_4]$ ([Li][**1**]), which as isolated as colorless plates in 20% yield (Scheme 1). We also sought to synthesize the analogous cerium(III) aryl complex $[Li(THF)_4][Ce(C_6Cl_5)_4]$ ([Li][**2**]), which was prepared by reaction of $[Ce(NO_3)_3(THF)_4]$ with 4 equiv of LiC_6Cl_5 in cold Et_2O (-25 °C) (Scheme 1). Work-up of the reaction mixture followed by recrystallization from concentrated toluene afforded [Li][**2**] as yellow plates in 16% yield. Importantly, [Li][**1**] and [Li][**2**] represent the first homoleptic perchlorophenyl complexes of the lanthanides.

The low yields observed for [Li][**1**] and [Li][**2**] reflect their high thermal sensitivity (see below). Indeed, the highest yields were achieved when the reaction time and temperature were minimized. In particular, reaction times were kept to 2 min, and the work-up was performed using cold pentane and toluene. Longer reaction times (e.g., 1 h at room temperature) resulted in substantially reduced yields. Attempts to improve the yields of [Li][**1**] and [Li][**2**] were met with limited success. For example, reaction of LiC_6Cl_5 with $CeCl_3$ or $[CeCl_3(THF)_4]$ did not generate [Li][**2**], likely because the low solubility of either starting material in Et_2O resulted in minimal conversion. In this regard, the successful use of $[Ln(NO_3)_3(THF)_4]$ in this chemistry likely reflects its higher solubility in Et_2O. Additionally, our choice of solvents was somewhat limited because LiC_6Cl_5 reacts rapidly with THF. Moreover, attempts to understand the mass balance of each transformation was complicated by the absence of a convenient NMR handle.

Scheme 1. Synthesis of Complexes [Li][**1**] and [Li][**2**]

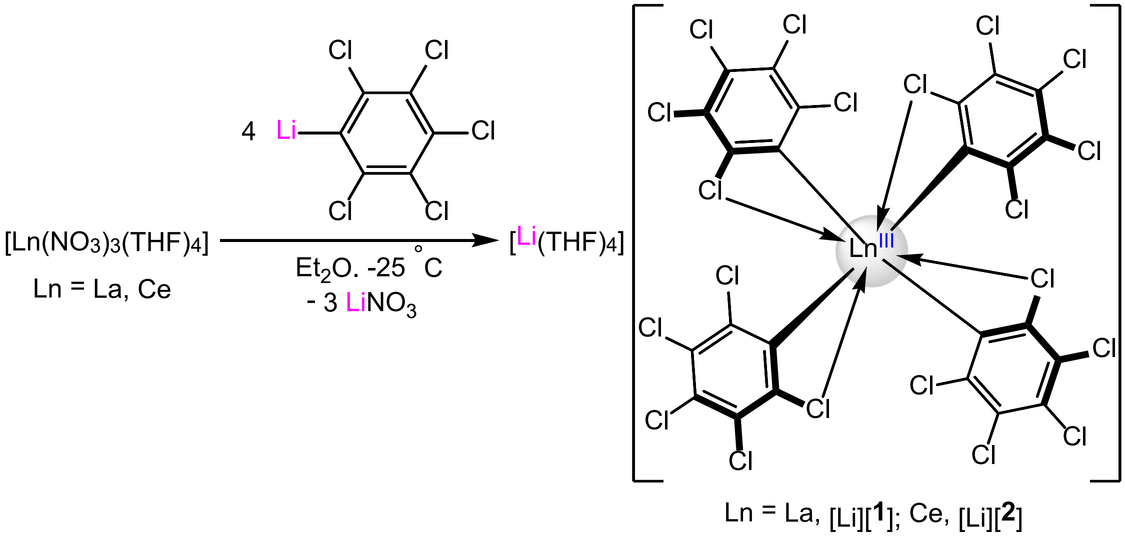

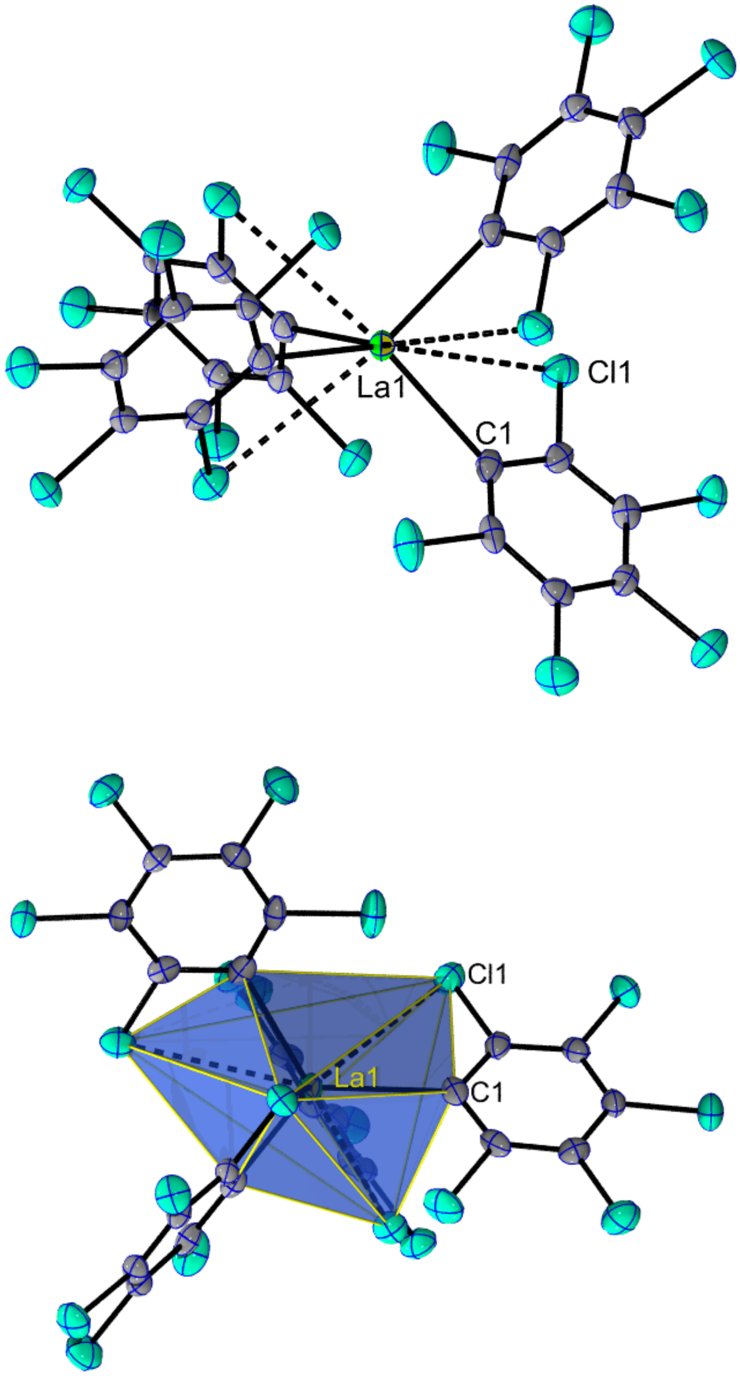

Figure 1. Solid-state molecular structure of [Li][**1**] shown with 50% probability ellipsoids (top). Solid-state molecular structure of [Li][**1**] with the triakis tetrahedron polygon shown in blue (bottom). The $[Li(THF)_4]^+$ counterion was omitted for clarity.

Complex [Li][**1**] crystallizes in the tetragonal space group $I4_1/a$ and features only one crystallographically independent aryl ligand (Figure 1). The eight-coordinate lanthanum center is coordinated by four *ipso* carbons and four "short" Ln—Cl contacts involving the *ortho*-Cl atoms of the C_6Cl_5 ligands. However, calculations suggest that the La center forms dative interactions of varying strengths with all eight *ortho*-Cl atoms (see below). According to the continuous shape measure,[34] the coordination geometry is best described as a T_d-symmetric triakis tetrahedron. Cl→M dative interactions were previously observed in $[Li(DME)_2(Et_2O)]_2[Li(DME)_2][Th(C_6Cl_5)_5]_3$ and $[Li(Et_2O)_4][U(C_6Cl_5)_5]$, as well as several transition metal examples.[14,15,19,24] Despite these nominally stabilizing interactions, [Li][**1**] still exhibits appreciable thermal sensitivity (see below). The La-C distance in [Li][**1**] is 2.594(3) Å (Table 1), which is similar to those seen in other σ-bonded lanthanum aryl complexes,[3,8,35] such as $[Cp_2La(2,6\text{-}(Me_2NCH_2)C_6H_3]$ (2.548(3) Å).[35] The Cl→Ln distance in [Li][**1**] (3.5193(9) Å) is significantly longer than the Cl→An interactions observed for $[Li(DME)_2(Et_2O)]_2[Li(DME)_2][Th(C_6Cl_5)_5]_3$ (av. 3.09 Å) and $[Li(Et_2O)_4][U(C_6Cl_5)_5]$ (av. 3.13 Å), despite their relatively similar ionic radii (i.e., La^{3+} = 1.032 Å; Th^{4+} = 0.94 Å; U^{4+} = 0.89 Å).[36]

Complex [Li][**2**] crystallizes in the monoclinic space group $P2_1/c$ as the toluene solvate, [Li][**2**]·C_7H_8 (Figure S3). The solid-state molecular structure of [Li][**2**] reveals an eight-coordinate cerium center formed by four Ln-C σ-bonds and four "short" Cl→Ln dative interactions. According to the continuous shape measure,[34] its coordination geometry is best described as a highly distorted triakis tetrahedron. The average Ce-C distance in [Li][**2**] is 2.559(7) Å (range = 2.542(7) – 2.579(7) Å; Table 1), which is shorter than the La-C distance in [Li][**1**], consistent with smaller ionic radius of the Ce(III) ion.[36] These values are also shorter than the $Ce\text{-}C_{ipso}$ distances in $[Cp'_2Ce(C_6F_5)]$ (Cp' = $1,2,4\text{-}{}^tBu_3C_5H_2$; 2.621(4) Å),[37] $[Cp'_2Ce(2,3,4,6\text{-}C_6HF_4)]$ (2.623(3) Å),[38] and [Cp'$_2$Ce(2,3,4,5-C_6HF_4)] (2.64(2) Å).[38] Interestingly, these examples also feature F→Ce dative interactions similar to the Cl→Ce interactions found in [Li][**2**].[39] In this regard, the "short" Cl→Ce distances in [Li][**2**] range from 3.455(2) to 3.558(2) Å. These values bracket that found in [Li][**1**].

Table 1. Selected metrical parameters for [Li][**1**] and [Li][**2**]·C_7H_8.

Complex	[Li][**1**]	[Li][**2**]·C_7H_8
Ln-C	2.594(3)	2.557(6), 2.542(7), 2.579(7), 2.552(7)
Cl→Ln	3.5193(9)	3.455(2), 3.470(2), 3.545(2), 3.558(2)
Ln-C_{ipso}-C_{ortho}	118.5(3)°, 126.1(2)°	118.8(5)°, 127.6(5)° 119.1(4)°, 126.1(5)° 120.3(5)°, 124.2(4)° 121.9(5)°, 123.0(5)°

Both [Li][**1**] and [Li][**2**] exhibit appreciable thermal sensitivity, as evidenced by a $^{13}C\{^1H\}$ NMR spectrum of an *in situ* prepared sample of [Li][**1**] that was allowed to stand at room temperature for 1 h (Figure S15). This spectrum reveals the formation of a number of decomposition products, including C_6Cl_5H, and while the other decomposition products could not be definitively identified, the number of peaks, and their positions, suggest that they could be chlorinated biphenyls.[40] Similar products are generated upon decomposition of Ln-C_6F_5 complexes.[11,39,41,42] Additionally, both [Li][**1**] and [Li][**2**] quickly decompose upon dissolution in tetrahydrofuran, CH_2Cl_2, pyridine, dimethoxyethane, and dimethylacetamide, as evidenced by the rapid formation of intractable deep orange-brown solutions. Isolated samples of [Li][**1**] and [Li][**2**] are insoluble hexanes and Et_2O, and only somewhat soluble in arene solvents. Curiously, however, the solubility of material prepared *in situ* in Et_2O is much improved. Accordingly, we recorded their $^{13}C\{^1H\}$ NMR spectra with material generated *in situ* in this solvent. These spectra were also recorded at -35 °C to minimize thermal decomposition. The *in situ* $^{13}C\{^1H\}$ NMR spectrum of complex [Li][**1**], recorded in a mixture of Et_2O/benzene-d_6, features a resonance at 185.41 ppm (Figure S6), which we assign to the *ipso* carbon environment of its pentachlorophenyl ligands. This resonance is much more upfield than the C_{ipso} resonances of $[Li(Et_2O)_2(THF)][UO_2(C_6Cl_5)_3]$[23] and $[Li(DME)_2(Et_2O)]_2[Li(DME)_2][Th(C_6Cl_5)_5]_3$,[24] which appear at 236.7 and 198.78 ppm, respectively, suggesting a much less covalent M-C interaction (see below for more discussion). This spectrum also features resonances at 139.80, 128.73, and 128.47 ppm, which we ascribe to the *ortho*, *meta*, and *para* resonances of the pentachlorophenyl ligand, respectively. Additionally, we observe resonances at 184.35, 141.06, 127.74, and 127.38 ppm, which we ascribe to the *ipso*, *ortho*, *meta*, and *para* resonances of unreacted LiC_6Cl_5, respectively. Confirmation of these assignments comes from a ^{13}C NMR spectrum of [Li][**1**] prepared with 10 equiv of LiC_6Cl_5 (Figure S8), as well as ^{13}C NMR spectrum of a sample of LiC_6Cl_5 prepared *in situ* (Figure S14). The *in situ* $^{13}C\{^1H\}$ NMR spectrum of [Li][**2**], recorded Et_2O/benzene-d_6, features a distinctive downfield resonance at 557.87 ppm (Figure S10), attributable to the *ipso* carbon of the pentachlorophenyl ligand. In addition, we observe resonances at 150.92, 149.83, and 129.66 ppm, which are assigned to the *ortho/meta*, *para*, and *ortho/meta* resonances of the pentachlorophenyl ligand, respectively. The large downfield shift of the C_{ipso} peak is consistent with the paramagnetism expected for [Li][**2**]. This spectrum also exhibits resonances assignable to unreacted LiC_6Cl_5.

Electronic Structure Analysis. To understand the electronic structures and bonding interactions within [Li][**1**] and [Li][**2**], DFT calculations with various hybrid and non-hybrid functionals, and a relativistic Hamiltonian, were performed on the anionic components, [**1**]$^-$ and [**2**]$^-$.[43–45]

Complete computational details are given in the Supporting Information. The calculated NMR shifts of [**1**]$^-$ were insensitive to the choice of functional, and therefore only the NMR data and corresponding bonding analysis obtained with the PBE functional are discussed in the following paragraphs. Complex [**1**]$^-$ is a closed-shell spin singlet, whereas complex [**2**]$^-$ exhibits a spin doublet configuration, as expected for a Ce(III) complex. The spin density is effectively localized at cerium, as evidenced by the Ce spin population of 0.986 (idealized 1.0) (Figure S1). The singly occupied molecular orbital (MO) is mostly of non-bonding 4f character. Natural localized MO (NLMO) analysis of the Ln-C$_{ipso}$ interactions reveals nearly identical orbital compositions for La and Ce (Figure 2), which is also indicated by the similar Ln-C$_{ipso}$ Wiberg bond orders (WBOs) of 0.30 and 0.33 for [**1**]$^-$ and [**2**]$^-$, respectively. The Ln weights in the σ-bonding NLMOs range from 8% (for [**1**]$^-$) to 9% (for [**2**]$^-$). Within these weights, the 4f and 5d contributions are 11% and 73% for [**1**]$^-$, respectively, and 17% and 69% for [**2**]$^-$, respectively, with the balance being 6s character in both cases (Table 2). The C$_{ipso}$ weights in the σ-bonding NLMOs are 84% for both [**1**]$^-$ and [**2**]$^-$. Within these weights, the 2s and 2p contributions are 25% and 75% for [**1**]$^-$, respectively, and 26% and 74% for [**2**]$^-$, respectively. In other words, there is an appreciable degree of donation bonding, but weaker than what is known from similar actinide complexes,[24,27,46] and the involvement of the 4f orbitals in the donation bonds is overall very minor. For comparison, the An-C$_{ipso}$ WBOs for $[An(C_6Cl_5)_5]^-$ are much larger, ranging from 0.47 for the Th analogue and 0.56 in the U analogue.[24] This difference reflects both the greater expected M-L covalency for the early actinides vs. the lanthanides, as well as the greater expected M-L covalency for M^{4+} vs M^{3+}.[32,47] The NLMO analysis of [**1**]$^-$ and [**2**]$^-$ also reveals the presence of eight weak Cl→An dative interactions in each complex. The average Ln weight in the NLMOs of these dative interactions is 2% for both [**1**]$^-$ and [**2**]$^-$ (Figure S2 and Table 1), which are commensurate with the experimentally measured (relatively long) Cl→Ln distances.

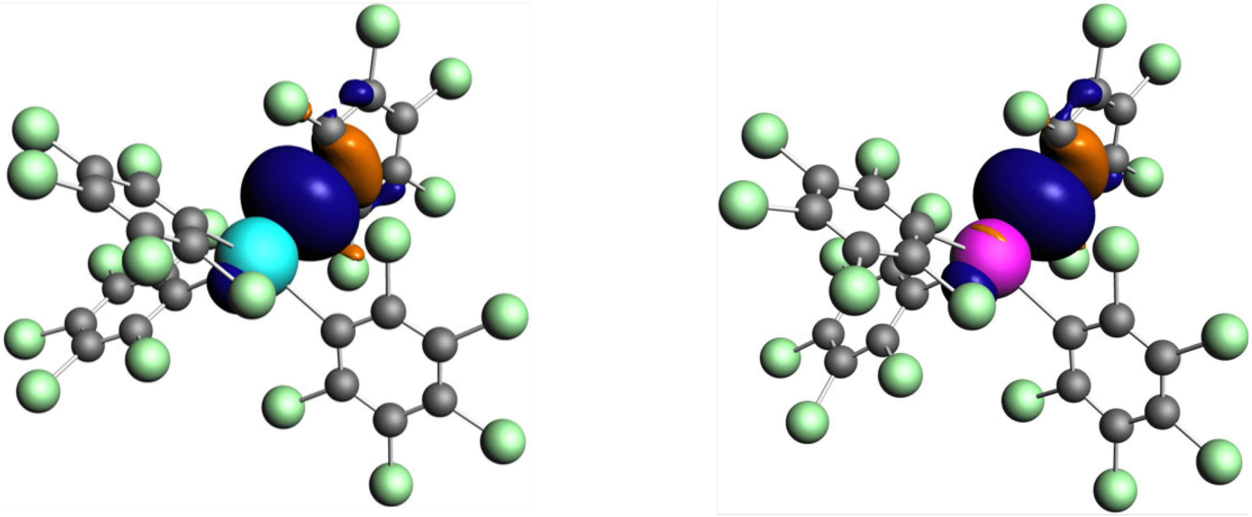

[**1**]$^-$ [**2**]$^-$

Figure 2. Representative Ln–C bonding NLMOs in [**1**]$^-$ and [**2**]$^-$. (Isosurface values ±0.03 au.)

Table 2. % weight compositions of the Ln-C (Ln = La, Ce) bonding and Lone pair (LP) NLMOs in [**1**]$^-$ and [**2**]$^-$. % orbital character averaged over equivalent NLMOs.

Complex	**Orbital**	**Total L**	***n*s**	***n*p**	**Total Ln**	**6s**	**5d**	**4f**
[**1**]$^-$	σ(La-C)	84	25	75	8	15	73	11
	LP(Cl)	96	26	74	2	19	76	5
[**2**]$^-$	σ(Ce-C)	84	26	74	9	14	69	17
	LP(Cl)	96	27	73	2	20	75	5

We calculated the ^{13}C NMR chemical shifts of the C_{ipso} nuclei for $[(Et_2O)_3Li(C_6Cl_5)]$ and [**1**]$^-$ with and without SO coupling effects. Repeated attempts to model the paramagnetic NMR (pNMR) ligand shifts for [**2**]$^-$ with DFT or wavefunction calculations were unsuccessful, likely because of a strong sensitivity of the spin delocalization and spin population to the dynamics of the system;[48–50] therefore, the chemical shifts for [**2**]$^{-}$ are not included in this analysis. The calculated C_{ipso}, C_{ortho}, C_{meta}, and C_{para} chemical shifts for $[(Et_2O)_3Li(C_6Cl_5)]$ are 180.9 ppm (exp = 183.63 ppm), 145.1 ppm (exp = 140.97 ppm), 132.6 ppm (exp = 127.79 ppm), and 131.7 ppm (exp = 127.57 ppm). These predictions match the experimental values reasonably well, and further confirm our assignments for the unreacted LiC_6Cl_5 in the *in situ* ^{13}C NMR spectra. The calculated C_{ipso}, C_{ortho}, C_{meta}, and C_{para} chemical shifts for [**1**]$^{-}$ are 184.0 ppm (exp = 185.41 ppm), 140.6 ppm (exp = 139.80 ppm), 131.6 ppm (exp = 128.73 ppm), and 132.3 ppm (exp = 128.47 ppm). These values, especially the C_{ipso} and C_{ortho} chemical shifts, are in excellent agreement with experiment.

The diamagnetic, paramagnetic, and spin-orbit shielding (σ) contributions to the C_{ipso} chemical shifts for both [**1**]$^{-}$ and $[Th(C_6Cl_5)_5]^{-}$ are provided in Table 3. Note, for both [**1**]$^{-}$ and $[Th(C_6Cl_5)_5]^{-}$, the 2s contributions to the M-C_{ipso} bonding are similar (25 and 28%, respectively).[24] Likewise, σ_d contributions are essentially identical and the σ_p contributions are very similar. The only substantive difference is the σ_{SO} contribution (-7.9 and -26.1 ppm, respectively), which can be explained by the greater covalency (and greater valence f-shell contributions) in the M-C_{ipso} donation bonds of $[Th(C_6Cl_5)_5]^{-}$ vs. [**1**]$^{-}$. $[Ce^{IV}(\kappa^2$-*ortho*-oxa$)(MBP)_2]^{-}$ features a large (40 ppm) deshielding due to SO coupling for the same reason.[32] Nonetheless, while the SO contribution to the C_{ipso} chemical shift in [**1**]$^{-}$ is relatively small, as expected given the weak 4f (and to a lesser extent 5d) participation in the La-C_{ipso} bonds, its inclusion is unequivocally necessary to achieve good agreement between theory and experiment.

Table 3. Calculated C_{ipso} NMR chemical shift (δ, in ppm) and individual isotropic shielding contributions (σ, in ppm) in [**1**]$^-$ and $[Th(C_6Cl_5)_5]^-$ at the SO-PBE level of theory.[a]

Compound	Method	σ_d	σ_p	σ_{so}	σ_{calc}	δ_{calc}	δ_{expt}	Ref
[**1**]$^-$	SO-PBE	248.7	-244.6	-7.9	-3.8	184.0	185.4	This work
$[Th(C_6Cl_5)_5]^-$	SO-PBE	248.4	-237.1	-26.1	-14.8	203.2	198.8	24

[a] σ_d, σ_p and σ_{so} indicate the diamagnetic, paramagnetic, and SO shielding, respectively, as partitioned in the NMR calculations.

Conclusion

In summary, we have prepared and characterized the first structurally authenticated homoleptic perchlorophenyl complexes of the lanthanides, $[Li(THF)_4][La(C_6Cl_5)_4]$ ([Li][**1**]) and $[Li(THF)_4][Ce(C_6Cl_5)_4]$ ([Li][**2**]), and we have confirmed their formulations by X-ray crystallography. A combined ^{13}C NMR spectroscopic and DFT study found that the Ln-C_{ipso} bonds are mostly ionic, with the donation bonding mainly involving the Ln 5d orbitals and only minimal 4f orbital participation. Indeed, the spin-orbit-induced deshielding of the C_{ipso} chemical shift was only ca. 8 ppm – much less than that calculated for comparable An^{4+} perchlorophenyl complexes. Yet, while the SO contribution to the C_{ipso} chemical shift is small, it must be included in the DFT calculations to accurately match theory to experiment, highlighting the sensitivity of this approach to unravel electronic structure.

ASSOCIATED CONTENT

Supporting Information. Experimental procedures, crystallographic details, computational results, and spectral data for complexes [Li][**1**] and [Li][**2**] (PDF).

AUTHOR INFORMATION

Corresponding Author

hayton@chem.ucsb.edu, jochena@buffalo.edu

ACKNOWLEDGEMENTS

This work was supported by the U.S. Department of Energy, Office of Basic Energy Sciences, Chemical Sciences, Biosciences, and Geosciences Division under Contract DE-SC0001861. This research made use of the 400 MHz NMR Spectrometer in the Department of Chemistry, an NIH SIG (1S10OD012077-01A1), and a 500 MHz NMR Spectrometer supported by an NSF Major Research Instrumentation (MRI) Award 1920299. J. A. acknowledges support for the theoretical component of this study by the U.S. Department of Energy, Office of Science, Heavy Element Chemistry program, grant DE-SC0001136. We thank the Center for Computational Research (CCR) at the University of Buffalo for providing computational resources.

References

(1) Petrov, A. R.; Thomas, O.; Harms, K.; Rufanov, K. A.; Sundermeyer, J. Dramatic Enhancement of the Stability of Rare-Earth Metal Complexes with α-Methyl Substituted N,N-Dimethylbenzylamine Ligands. *J. Organomet. Chem.* **2010**, *695*, 2738–2746.

(2) Cotton, S. A.; Hart, F. A.; Hursthouse, M. B.; Welch, A. J. Preparation and Molecular Structure of a σ-Bonded Lanthanide Phenyl. *J. Chem. Soc., Chem. Commun.* **1972**, 1225–1226.

(3) Pan, Y.; Xu, T.; Yang, G.-W.; Jin, K.; Lu, X.-B. Bis(oxazolinyl)phenyl-Ligated Rare-Earth-Metal Complexes: Highly Regioselective Catalysts for Cis-1,4-Polymerization of Isoprene. *Inorg. Chem.* **2013**, *52*, 2802–2808.

(4) Petrov, A. R.; Rufanov, K. A.; Harms, K.; Sundermeyer, J. Re-Investigation of Ortho-Metalated N,N-Dialkylbenzylamine Complexes of Rare-Earth Metals. First Structurally Characterized Arylates of Neodymium and Gadolinium Li[LnAr$_4$]. *J. Organomet. Chem.* **2009**, *694*, 1212–1218.

(5) Zimmermann, M.; Anwander, R. Homoleptic Rare-Earth Metal Complexes Containing Ln−C σ-Bonds. *Chem. Rev.* **2010**, *110*, 6194–6259.

(6) Ihara, E.; Adachi, Y.; Yasuda, H.; Hashimoto, H.; Kanehisa, N.; Kai, Y. Synthesis of 2,6-Dialkoxylphenyllanthanoid Complexes and Their Polymerization Catalysis. *J. Organomet. Chem.* **1998**, *569*, 147–157.

(7) Wayda, A. L.; Atwood, J. L.; Hunter, W. E. Homoleptic Organolanthanoid Hydrocarbyls. The Synthesis and X-Ray Crystal Structure of Tris[o-((dimethylamino)methyl)phenyl]lutetium. *Organometallics* **1984**, *3*, 939–941.

(8) Martinez-Arripe, E.; Jean-Baptiste-dit-Dominique, F.; Auffrant, A.; Le Goff, X.-F.; Thuilliez, J.; Nief, F. Synthesis and Characterization of Bidentate Rare-Earth Iminophosphorane *o*-Aryl Complexes and Their Behavior As Catalysts for the Polymerization of 1,3-Butadiene. *Organometallics* **2012**, *31*, 4854–4861.

(9) Bochkarev, L. N.; Stepantseva, T. A.; Zakharov, L. N.; Fukin, G. K.; Yanovsky, A. I.; Struchkov, Y. T. Synthesis and Crystal Structure of $Ph_3Ln(THF)_3$ (Ln = Er, Tm). *Organometallics* **1995**, *14*, 2127–2129.

(10) Forsyth, C. M.; Deacon, G. B. The First Crystallographically Characterized (Perfluoroaryl)lanthanoid(II) Complex, $Eu(C_6F_5)_2(OC_4H_8)_5$. *Organometallics* **2000**, *19*, 1205–1207.

(11) Deacon, G. B.; Forsyth, C. M. A Half-Sandwich Perfluoroorganoytterbium(II) Complex from a Simple Redox Transmetalation/Ligand Exchange Synthesis. *Organometallics* **2003**, *22*, 1349–1352.

(12) Heckmann, G.; Niemeyer, M. Synthesis and First Structural Characterization of Lanthanide(II) Aryls: Observation of a Schlenk Equilibrium in Europium(II) and Ytterbium(II) Chemistry. *J. Am. Chem. Soc.* **2000**, *122*, 4227–4228.

(13) Ara, I.; Forniés, J.; García-Monforte, M. A.; Martín, A.; Menjón, B. Synthesis and Characterization of Pentachlorophenyl–Metal Derivatives with d^0 and d^{10} Electron Configurations. *Chem. Eur. J.* **2004**, *10*, 4186–4197.

(14) Forniés, J.; Menjón , B.; Sanz-Carrillo, R. M.; Tomás, M.; Connelly, N. G.; Crossley, J. G.; Orpen, A. G. Synthesis and Structural Characterization of the First Isolated Homoleptic Organoplatinum(IV) Compound: $[Pt(C_6Cl_5)_4]$. *J. Am. Chem. Soc.* **1995**, *117*, 4295–4304.

(15) García, M. P.; Jiménez, M. V.; Lahoz, F. J.; López, J. A.; Oro, L. A. Synthesis of the Homoleptic Rhodium(III) Complex [Rh(C_6Cl_5)$_3$]. Molecular Structures of [Rh(C_6Cl_5)$_3$] and [Rh(C_6Cl_4–C_6Cl_4)(C_6Cl_5)(SC_4H_8)$_2$]. *J. Chem. Soc., Dalton Trans.* **1998**, 4211–4214.

(16) García, M. P.; Jiménez, M. V.; Oro, L. A.; Lahoz, F. J.; Tiripicchio, M. C.; Tiripicchio, A. A Homoleptic Mononuclear Iridium(II) Organometallic Complex: Synthesis and X-Ray Structure of $[Ir(C_6Cl_5)_4]^{2-}$. *Organometallics* **1993**, *12*, 4660–4663.

(17) Alonso, P. J.; Forniés, J.; García-Monforte, M. A.; Martín, A.; Menjón, B. The First Structurally Characterised Homolepticorganovanadium(III) Compound. *Chem. Commun.* **2001**, 2138–2139.

(18) Alonso, P. J.; Falvello, L. R.; Forniés, J. Synthesis and First Structural Characterisation of a Homoleptic Tetraorganochromate(III) Salt. *Chem. Commun.* **1998**, 1721–1722.

(19) Alonso, P. J.; Forniés, J.; García-Monforte, M. A.; Martín, A.; Menjón, B.; Rillo, C. A New Series of Homoleptic, Paramagnetic Organochromium Derivatives: Synthesis, Characterization, and Study of Their Magnetic Properties. *Chem. Eur. J.* **2002**, *8*, 4056–4065.

(20) Alonso, P. J.; Arauzo, A. B.; Forniés, J.; García-Monforte, M. A.; Martín, A.; Martínez, J. I.; Menjón, B.; Rillo, C.; Sáiz-Garitaonandia, J. J. A Square-Planar Organoiron(III) Compound with a Spin-Admixed State. *Angew. Chem. Int. Ed.* **2006**, *45*, 6707–6711.

(21) Alonso, P. J.; Forniés, J.; García-Monforte, M. A.; Martín, A.; Menjón, B. New Homoleptic Organometallic Derivatives of Vanadium(III) and Vanadium(IV): Synthesis, Characterization, and Study of Their Electrochemical Behaviour. *Chem. Eur. J.* **2005**, *11*, 4713–4724.

(22) García-Monforte, M. A.; Alonso, P. J.; Forniés, J.; Menjón, B. New Advances in Homoleptic Organotransition-Metal Compounds: The Case of Perhalophenyl Ligands. *Dalton Trans.* **2007**, 3347–3359.

(23) Ordoñez, O.; Yu, X.; Wu, G.; Autschbach, J.; Hayton, T. W. Synthesis and Characterization of Two Uranyl-Aryl "Ate" Complexes. *Chem. Eur. J.* **2021**, *27*, 5885–5889.

(24) Ordoñez, O.; Yu, X.; Wu, G.; Autschbach, J.; Hayton, T. W. Homoleptic Perchlorophenyl "Ate" Complexes of Thorium(IV) and Uranium(IV). *Inorg. Chem.* **2021**, *60*, 12436–12444.

(25) Kent, G. T.; Yu, X.; Pauly, C.; Wu, G.; Autschbach, J.; Hayton, T. W. Synthesis of Parent Acetylide and Dicarbide Complexes of Thorium and Uranium and an Examination of Their Electronic Structures. *Inorg. Chem.* **2021**, *60*, 15413–15420.

(26) Kent, G. T.; Yu, X.; Wu, G.; Autschbach, J.; Hayton, T. W. Synthesis and Electronic Structure Analysis of the Actinide Allenylidenes, $[\{(NR_2)_3\}An(CCCPh_2)]^{-}$ (An = U, Th; R = $SiMe_3$). *Chem. Sci.* **2021**, *12*, 14383–14388.

(27) Pedrick, E. A.; Hrobárik, P.; Seaman, L. A.; Wu, G.; Hayton, T. W. Synthesis, Structure and Bonding of Hexaphenyl Thorium(IV): Observation of a Non-Octahedral Structure. *Chem. Commun.* **2016**, *52*, 689–692.

(28) Mullane, K. C.; Hrobárik, P.; Cheisson, T.; Manor, B. C.; Carroll, P. J.; Schelter, E. J. ^{13}C NMR Shifts as an Indicator of U–C Bond Covalency in Uranium(VI) Acetylide Complexes: An Experimental and Computational Study. *Inorg. Chem.* **2019**, *58*, 4152–4163.

(29) Smiles, D. E.; Wu, G.; Hrobárik, P.; Hayton, T. W. Synthesis, Thermochemistry, Bonding, and ^{13}C NMR Chemical Shift Analysis of a Phosphorano-Stabilized Carbene of Thorium. *Organometallics* **2017**, *36*, 4519–4524.

(30) Seaman, L. A.; Hrobárik, P.; Schettini, M. F.; Fortier, S.; Kaupp, M.; Hayton, T. W. A Rare Uranyl(VI)–Alkyl Ate Complex $[Li(DME)_{1.5}]_2[UO_2(CH_2SiMe_3)_4]$ and Its Comparison with a Homoleptic Uranium(VI)–Hexaalkyl. *Angew. Chem. Int. Ed.* **2013**, *52*, 3259–3263.

(31) Kent, G. T.; Yu, X.; Wu, G.; Autschbach, J.; Hayton, T. W. Ring-Opening of a Thorium Cyclopropenyl Complex Generates a Transient Thorium-Bound Carbene. *Chem. Commun.* **2022**, *58*, 6805–6808.

(32) Panetti, G. B.; Sergentu, D.-C.; Gau, M. R.; Carroll, P. J.; Autschbach, J.; Walsh, P. J.; Schelter, E. J. Isolation and Characterization of a Covalent Ce^{IV}-Aryl Complex with an Anomalous ^{13}C Chemical Shift. *Nat. Commun.* **2021**, *12*, 1713.

(33) Rausch, M. D.; Tibbetts, F. E.; Gordon, H. B. Perhaloaryl-Metal Chemistry: II. Pentachlorophenyllithium. *J. Organomet. Chem.* **1966**, *5*, 493–500.

(34) Cirera, J.; Ruiz, E.; Alvarez, S. Continuous Shape Measures as a Stereochemical Tool in Organometallic Chemistry. *Organometallics* **2005**, *24*, 1556–1562.

(35) Hogerheide, M. P.; Boersma, J.; Spek, A. L.; van Koten, G. Synthesis of a Bis(cyclopentadienyl)lanthanum Aryl Complex with a Pseudofacially Bound Bis(ortho)-Chelating Aryldiamine Ligand. X-Ray Structure of $(\eta^5\text{-}C_5H_5)_2La(C_6H_3\{CH_2NMe_2\}_2\text{-}2,6)$. *Organometallics* **1996**, *15*, 1505–1507.

(36) Shannon, R. D. Revised Effective Ionic Radii and Systematic Studies of Interatomic Distances in Halides and Chalcogenides. *Acta Cryst A* **1976**, *32*, 751–767.

(37) Maron, L.; Werkema, E. L.; Perrin, L.; Eisenstein, O.; Andersen, R. A. Hydrogen for Fluorine Exchange in C_6F_6 and C_6F_5H by Monomeric $[1,3,4\text{-}(Me_3C)_3C_5H_2]_2CeH$: Experimental and Computational Studies. *J. Am. Chem. Soc.* **2005**, *127*, 279–292.

(38) Werkema, E. L.; Andersen, R. A. Fluorine for Hydrogen Exchange in the Hydrofluorobenzene Derivatives $C_6H_xF_{(6-x)}$, Where x = 2, 3, 4 and 5 by Monomeric $[1,2,4\text{-}(Me_3C)_3C_5H_2]_2CeH$: The Solid State Isomerization of $[1,2,4\text{-}(Me_3C)_3C_5H_2]_2Ce(2,3,4,5\text{-}C_6HF_4)$ to $[1,2,4\text{-}(Me_3C)_3C_5H_2]_2Ce(2,3,4,6\text{-}C_6HF_4)$. *J. Am. Chem. Soc.* **2008**, *130*, 7153–7165.

(39) Yin, H.; Zabula, A. V.; Schelter, E. J. C–F→Ln/An Interactions in Synthetic f-Element Chemistry. *Dalton Trans.* **2016**, *45*, 6313–6323.

(40) Yanagisawa, M.; Hayamizu, K.; Yamamoto, O. ^{13}C Chemical Shifts of Chlorinated Biphenyls. *Magn. Reson. Chem.* **1986**, *24*, 1013–1014.

(41) Deacon, G. B.; Jaroschik, F.; Junk, P. C.; Kelly, R. P. A Divalent Heteroleptic Lanthanoid Fluoride Complex Stabilised by the Tetraphenylcyclopentadienyl Ligand, Arising from C–F Activation of Pentafluorobenzene. *Chem. Commun.* **2014**, *50*, 10655–10657.

(42) Deacon, G. B.; Koplick, A. J.; Raverty, W. D.; Vince, D. G. Organolanthanoids: II. Preparation and Identification of Some Organolanthanoid Species in Solution. *J. Organomet. Chem.* **1979**, *182*, 121–141.

(43) Glendening, E. D.; Landis, C. R.; Weinhold, F. NBO 6.0: Natural Bond Orbital Analysis Program. *J. Comput. Chem.* **2013**, *34*, 1429–1437.

(44) Autschbach, J. The Role of the Exchange-Correlation Response Kernel and Scaling Corrections in Relativistic Density Functional Nuclear Magnetic Shielding Calculations with the Zeroth-Order Regular Approximation. *Mol. Phys.* **2013**, *111*, 2544–2554.

(45) E. J. Baerends, T. Ziegler, A. J. Atkins, J. Autschbach, O. Baseggio, D. Bashford, A. Bérces, F. M. Bickelhaupt, C. Bo, P. M. Boerrigter, L. Cavallo, C. Daul, D. P. Chong, D. V. Chulhai, L. Deng, R. M. Dickson, J. M. Dieterich, D. E. Ellis, M. v. Faassen, L. Fan, T. H. Fischer, C. F. Guerra, M. Franchini, A. Ghysels, A. Giammona, S. J. A. v. Gisbergen, A. Goez,; A. W. Götz, J. A. Groeneveld, O. V. Gritsenko, M. Grüning, S. Gusarov, F. E. Harris, P. v. d. Hoek, Z. Hu, C. R. Jacob, H. Jacobsen, L. Jensen, L. Joubert, J. W. Kaminski, G. v. Kessel, C. König, F. Kootstra, A. Kovalenko, M. V. Krykunov, E. v. Lenthe, D. A. McCormack, A. Michalak, M. Mitoraj, S. M. Morton, J. Neugebauer, V. P. Nicu, L. Noodleman, V. P. Osinga, S. Patchkovskii, M. Pavanello, C. A. Peeples, P. H. T. Philipsen, D. Post, C. C. Pye, H. Ramanantoanina, P. Ramos, W. Ravenek, J. I. Rodríguez, P. Ros, R. Rüger, P. R. T. Schipper, D. Schlüns, H. v. Schoot, G. Schreckenbach, J. S. Seldenthuis, M. Seth, J. G. Snijders, M. Solà, M. Stener, M. Swart, D. Swerhone, V. Tognetti, G. t. Velde, P. Vernooijs, L. Versluis, L. Visscher, O. Visser, F. Wang, T. A. Wesolowski, E. M. v. Wezenbeek, G. Wiesenekker, S. K. Wolff, T. K. Woo, A. L. Yakovlev, Amsterdam Density Functional. 2017 Ed.; SCM, Theoretical Chemistry, Vrije Universiteit Amsterdam, The Netherlands, 2017. https://www.scm.com.

(46) Wolford, N. J.; Sergentu, D.-C.; Brennessel, W. W.; Autschbach, J.; Neidig, M. L. Homoleptic Aryl Complexes of Uranium (IV). *Angew. Chem. Int. Ed.* **2019**, *58*, 10266–10270.

(47) Löble, M. W.; Keith, J. M.; Altman, A. B.; Stieber, S. C. E.; Batista, E. R.; Boland, K. S.; Conradson, S. D.; Clark, D. L.; Lezama Pacheco, J.; Kozimor, S. A.; Martin, R. L.; Minasian, S. G.; Olson, A. C.; Scott, B. L.; Shuh, D. K.; Tyliszczak, T.; Wilkerson, M. P.; Zehnder, R. A. Covalency in Lanthanides. An X-Ray Absorption Spectroscopy and Density Functional Theory Study of $LnCl_6^{x-}$ (x = 3, 2). *J. Am. Chem. Soc.* **2015**, *137*, 2506–2523.

(48) Martin, B.; Autschbach, J. Temperature Dependence of Contact and Dipolar NMR Chemical Shifts in Paramagnetic Molecules. *J. Chem. Phys.* **2015**, *142*, 054108.

(49) Gendron, F.; Sharkas, K.; Autschbach, J. Calculating NMR Chemical Shifts for Paramagnetic Metal Complexes from First-Principles. *J. Phys. Chem. Lett.* **2015**, *6*, 2183–2188.

(50) Autschbach, J. Chapter One - NMR Calculations for Paramagnetic Molecules and Metal Complexes. In *Annual Reports in Computational Chemistry*; Dixon, D. A., Ed.; Elsevier, 2015; Vol. 11, pp 3–36.

Table of Contents

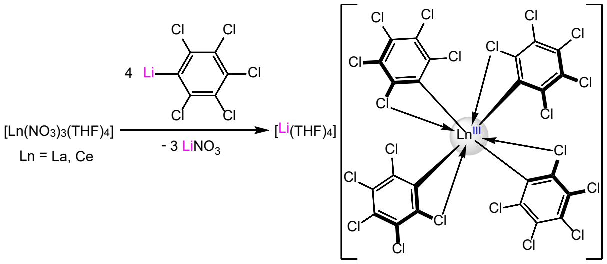

The homoleptic lanthanide-aryl "ate" complexes, $[Li(THF)_4][Ln(C_6Cl_5)_4]$ (Ln = La, Ce), exhibit highly ionic Ln-C_{ipso} bonds with minimal 4f orbital participation, according to a combined ^{13}C NMR spectroscopic and density functional theory study.